Journal of Applied Mechanics and Technical Physics, Vol. 48, No. 6, pp. 795–812, 2007

MODIFIED SHALLOW WATER EQUATIONS WHICH ADMIT THE PROPAGATION OF DISCONTINUOUS WAVES OVER A DRY BED

V. V. Ostapenko

UDC 519.63

A method for modeling the propagation of discontinuous waves over a dry bed using the first approximation of shallow water theory is proposed. The method is based on a modified conservation law of total momentum that takes into account the concentrated momentum losses due to the formation of local turbulent vortex structures in the fluid surface layer at a discontinuous-wave front. A quantitative estimate of these losses is obtained by deriving the shallow water equations from the Navier–Stokes equations with allowance for viscosity, which has a rapidly increasing effect in the turbulent flow regions described by discontinuous waves. The stability of the discontinuous waves admitted by the modified system of conservation laws of shallow water theory is examined. As an example, a comparative analysis is performed of the solutions of the dam-break problem obtained for the classical and modified shallow water models.

Key words: *shallow water equations, discontinuous waves, modified total-momentum conservation law, dam-break problem.*

Introduction. The equations of the first approximation of shallow water theory [1–5] are widely used to model the propagation of discontinuous waves [6–8] (hydraulic bores [9–11]) generated by total or partial dam breaks or by the impact of large sea tsunami-type waves [12] on shallow water. As is known, the classical system of the basic conservation laws of shallow water theory, consisting of the conservation laws for mass and total momentum [3–5], while correctly describing the parameters of discontinuous waves propagating in a fluid of finite depth [1], does not admit discontinuous-wave propagation over a dry bed. The exact solutions describing water flow over a dry bed within the framework of this system are continuous depression waves (a simple example of such a wave generated by dam break above a horizontal bottom was first constructed in [13]). Accounting for bottom friction, which is a distributed source term making no contribution to the Hugoniot conditions at a discontinuous wave front, cannot change this situation [14–17]. At the same time, numerous laboratory experiments have shown that these continuous solutions considerably overestimate the propagation velocity of the wave leading edge and distorts the wave profile [18–23]. In experiments, the waves propagating over a dry bed have a significantly steeper front, on which breaks characteristic of discontinuous waves occur.

Figure 1a gives a photograph of the wave obtained in laboratory modeling of the dam-break problem with a dry bed in the tailwater. The wave flow is produced by a sudden removal of the flat shield bounding the stationary fluid in the headwater (a detailed description of the results of the experiment is given in [21, 23]). From the results of the experiments, it follows that the head of the moving wave had a pulsating and quasistationary profile (Fig. 1b). The hydraulic jump BC, incoming on the thin water layer AB propagating ahead, gradually absorbs some of its part. The steepness of the leading edge of the jump BC thus decreases. As a result, the jump is almost completely degenerated and the free surface profile at the wave head becomes fairly flat. Next, the reverse process occurs: the free surface profile at the wave head at some distance from its edge gradually becomes steeper, which leads to the formation of a new hydraulic jump of the form of BC. At the same time, the water strip AB ahead of the front of

Lavrent'ev Institute of Hydrodynamics, Siberian Division, Russian Academy of Sciences, Novosibirsk 630090; ostapenko_vv@ngs.ru. Translated from Prikladnaya Mekhanika i Tekhnicheskaya Fizika, Vol. 48, No. 6, pp. 22–43, November–December, 2007. Original article submitted February 7, 2006; revision submitted November 23, 2006.

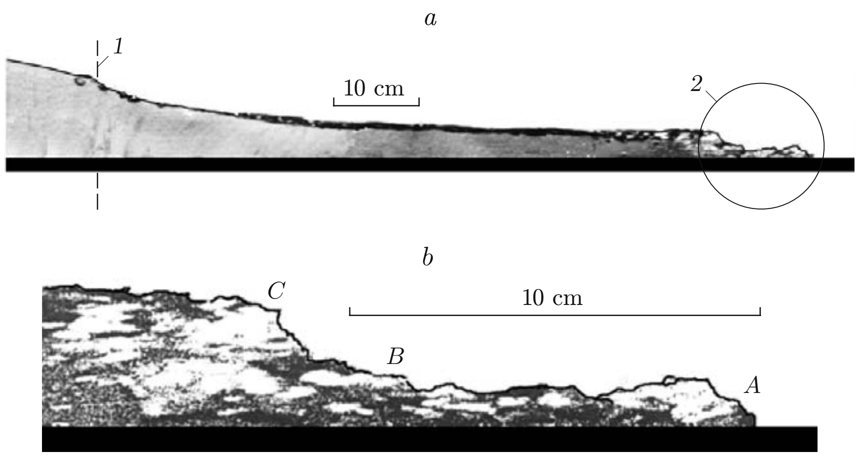

Fig. 1. Wave obtained in laboratory modeling of the dam-break problem with a dry bed in the tailwater: (a) general view: position of the flat shield specifying the initial level difference (1) and wave head (2); (b) wave head (AB is a thin layer and BC is a hydraulic jump).

this jump is elongated and becomes thinner. As a result, the wave head takes the original shape (Fig. 1b). Next, this process occurs periodically.

In the present paper, the wave-head flow over a dry bed described above is modeled as a discontinuous wave propagating over a dry bed using the first approximation of shallow water theory. This modeling approach is based on a modified law of conservation of total momentum that takes into account the concentrated momentum losses due to the formation of local turbulent vortex structures at discontinuous-wave fronts. A quantitative estimate of these losses is obtained by deriving the shallow water equations from the Navier–Stokes equations with allowance for the viscosity, which has a rapidly increasing effect in the turbulent flow regions described by discontinuous waves. The heuristic parameter appearing in this case is chosen so as to provide good agreement with results of laboratory experiments [21–23]. The stability of the discontinuous waves admitted by the modified system of the conservation laws of shallow water theory is studied. As an example, a comparative analysis is performed of the solutions of the dam-break problem obtained for the classical and modified shallow water models. The analysis shows that, compared to the classical model, the modified model provides a much better fit to the average experimental parameters of the waves propagating over a dry bed. At the same time, a detailed description of the pulsating quasi-stationary processes at the wave head requires the use of higher-level models.

1. Basic Conservation Laws of Shallow Water Theory. In the case of a rectangular horizontal bed of constant width ignoring bottom friction, the basic conservation laws of shallow water theory [1–5] are written as

$$h_t + q_x = 0; \tag{1.1}$$

$$q_t + (qu + gh^2/2)_x = 0, \tag{1.2}$$

where $h(x,t)$, $q(x,t)$, and $u = q/h$ are the flow depth, flow rate, and fluid velocity, respectively, and g is the acceleration due to gravity. Equations (1.1) and (1.2) are differential forms of the physical conservation laws for mass and total momentum [5]. Equations (1.1) and (1.2) lead to the Hugoniot conditions at the discontinuous-wave front:

$$D[h] = [q]; \tag{1.3}$$

$$D[q] = [qu + gh^2/2]. \tag{1.4}$$

Here $D = x_t$ is the wave propagation velocity and $[f] = f_1 - f_0$ is the jump of the function f at the wave front $x = x(t)$:

$$f_0 = f(x(t)+0,t), \qquad f_1 = f(x(t)-0,t).$$

The average value of the function f at the discontinuous-wave front will be denoted by

$$\langle f \rangle = (f_0 + f_1)/2. \tag{1.5}$$

Then, from the Hugoniot condition (1.3) for the mass conservation law (1.1), we have

$$D - \langle u \rangle = [q]/[h] - \langle u \rangle = \langle h \rangle [u]/[h]. \tag{1.6}$$

Because, in view of (1.5) and (1.6), we have

$$D[q] - [qu] = (D - \langle u \rangle)[q] - \langle q \rangle [u] = (\langle h \rangle [q] - \langle q \rangle [h])[u]/[h] = (h_0 q_1 - h_1 q_0)[u]/[h].$$

From the Hugoniot condition (1.4) for the total-momentum conservation law (1.2) and the relation $[h^2/2] = (h_1^2 - h_0^2)/2 = \langle h \rangle [h]$, we obtain

$$(h_0 q_1 - h_1 q_0)[u]/[h] = h_0 h_1 [u]^2/[h] = g\langle h \rangle [h]. \tag{1.7}$$

Formula (1.7) implies that the velocity jump $[u]$ and the depth jump $[h]$ at the discontinuous-wave front are related by the condition

$$[u] = B_1(h_0, h_1)[h], \tag{1.8}$$

where

$$B_1(h_0, h_1) = \sqrt{g\langle h \rangle/(h_0 h_1)} = \sqrt{g(h_0 + h_1)/(2h_0 h_1)}. \tag{1.9}$$

Because

$$\lim_{h_0 \to 0} B_1(h_0, h_1) = +\infty,$$

system (1.1), (1.2) does not admit the propagation finite-amplitude discontinuous waves over a dry bed in which the depth ahead of the wave front $h_0 = 0$. As shown in Sec. 2, The reason for this is that the classical total-momentum conservation law (1.2) ignores the concentrated source term responsible for the total-momentum losses at the discontinuous-wave front.

2. Discontinuous Waves Propagating over a Dry Bed and Their Stability. In the Hugoniot condition (1.3) for the mass conservation law (1.1), we set

$$h_0 = u_0 = 0, \qquad h_1 > 0. \tag{2.1}$$

This implies that a discontinuous wave propagates over a dry bed. Substitution of values (2.1) into condition (1.3) yields

$$D h_1 = q_1 = h_1 u_1 \quad \Rightarrow \quad D = u_1, \tag{2.2}$$

i.e., the propagation velocity of this discontinuous waves coincides with the fluid velocity behind its front.

The system of shallow water equations (2.1), (2.2), like any other hyperbolic system of the second order [5], admits an infinite number of linearly independent conservation laws

$$\frac{\partial U(h,u)}{\partial t} + \frac{\partial F(h,u)}{\partial x} = 0. \tag{2.3}$$

If the conservation law (2.3) is incompatible with the mass conservation law (1.1) for discontinuous waves (2.2) propagating over a dry bed (2.1), then, in view of the normalization $U(0,0) = F(0,0) = 0$, the disbalance δU of the quantity $U(h,u)$ at the front of such a wave is calculated from the formula

$$\delta U = D[u] - [F] = u_1 U(h_1, u_1) - F(h_1, u_1). \tag{2.4}$$

For $\delta U > 0$, the quantity $U(h,u)$ on the discontinuous wave increases, and for $\delta U < 0$, it decreases. Applying formula (2.4) to the total-momentum conservation law (1.2), we obtain the relation

$$\delta q = -g h_1^2/2, \tag{2.5}$$

from which it follows that on the discontinuous wave (2.2) propagating over the dry bed (2.1), there is a total-momentum loss ($\delta q < 0$).

To justify such losses theoretically, we consider the total-energy conservation law

$$e_t + (eu + ghq/2)_x = 0, \tag{2.6}$$

where $e = (qu + gh^2)/2$ is the total energy of the flow, which, in shallow water theory, is the sum of the kinetic energy $e_k = qu/2 = hu^2/2$ and potential energy $e_p = gh^2/2$ [5]. For smooth solutions, Eq. (2.6) is a differential corollary of the basic system (1.1), (1.2). To derive this equation, it is necessary to multiply Eq. (1.1) by u and subtract the result from Eq. (1.2). As a result, dividing by h, we obtain the following equation for the change in the local momentum of each particle of the fluid:

$$u_t + (u^2/2 + gh)_x = 0. \tag{2.7}$$

Combining Eq. (2.7) multiplied by $q/2$ and Eq. (1.2) multiplied by $u/2$, we obtain the equation describing the change in the kinetic energy e_k:

$$(e_k)_t + (ue_k)_x + gqh_x = 0. \tag{2.8}$$

Combining Eq. (2.8) and Eq. (1.1) multiplied by gh, we finally obtain the differential form (2.6) of the total-energy conservation law, for which the Hugoniot condition is given by

$$D[e] = [ue + ghq/2]. \tag{2.9}$$

Applying formula (2.4) to the total-energy conservation law (2.6), we obtain the relation

$$\delta e = -gh_1^2 u_1/2, \tag{2.10}$$

which implies that for

$$u_1 = D > 0 \tag{2.11}$$

on the discontinuous wave (2.2) propagating over the dry bed (2.1), there is a loss of the total energy of the incoming flow ($\delta e < 0$). For

$$u_1 = D < 0 \tag{2.12}$$

the total energy on the discontinuous wave (2.1), (2.2) increases ($\delta e > 0$).

If the shallow water equations are considered in terms of the general theory of hyperbolic systems of conservation laws with a convex expansion [24, 25], the total-energy conservation law is a closing convex conservation law and the total-energy loss at discontinuities ($\delta e < 0$) is therefore the entropic [25] (energetic [5]) stability criterion for discontinuous waves. In view of this, the discontinuous wave (2.2), propagating over the dry bed (2.1) is stable if condition (2.11) is satisfied, and it is unstable if condition (2.12) holds.

In shallow water theory, the total-energy loss on discontinuous waves can be treated as a process in which part of this energy in real flow is converted to the energy of small-scale vortices. In the classical case, these vortices are moved upstream of the wave front, where they are gradually damped under the action of viscosity. In the flows described by discontinuous waves propagating over a dry bed, this vortex motion, by virtue of condition (2.2), is localized at the wave front, and, in view of the equality $\delta e = u_1 \delta q$ implied by (2.5) and (2.10), the energy δe converted to this motion is totally expended in the incoming-flow deceleration related to the loss of its total momentum.

The discontinuous waves (2.1), (2.2), and (2.11) formally also satisfy the evolutionary [4] (characteristic [5, 23]) stability condition

$$\lambda_s^1 > D > \lambda_s^0 \geq \lambda_r^0, \qquad D > \lambda_r^1, \tag{2.13}$$

where $\lambda_r^0 = u_0 - c_0 = 0$ and $\lambda_s^0 = u_0 + c_0 = 0$ are the velocities of the r- and s-characteristics ahead of the wave front in the dry bed area $h_0 = u_0 = 0$ and $\lambda_r^1 = u_1 - c_1$ and $\lambda_s^1 = u_1 + c_1$ are the velocities of the r- and s-characteristics behind the discontinuous-wave front, respectively. The r-invariant ($r = u - 2c$) is conserved along the r-characteristics, and the s-invariant ($s = u + 2c$) along the s-characteristics ($c = \sqrt{gh}$ is the propagation velocity of small perturbations in shallow water theory [5]). Inequalities (2.13) imply that three characteristics λ_r^0, λ_s^0, and λ_s^1 arrive at the front of the stable discontinuous wave (2.1), (2.2), (2.11), and only one λ_r^1-characteristic leaves it. Similarly, it can be shown that the discontinuous waves (2.1), (2.2), (2.12) unstable under the energetic criterion do not also satisfy the characteristic stability condition (2.13).

Below a modified total-momentum conservation law is obtained which takes into account the concentrated momentum losses due to local flow transition to turbulence in the fluid surface layer at the discontinuous-wave front.

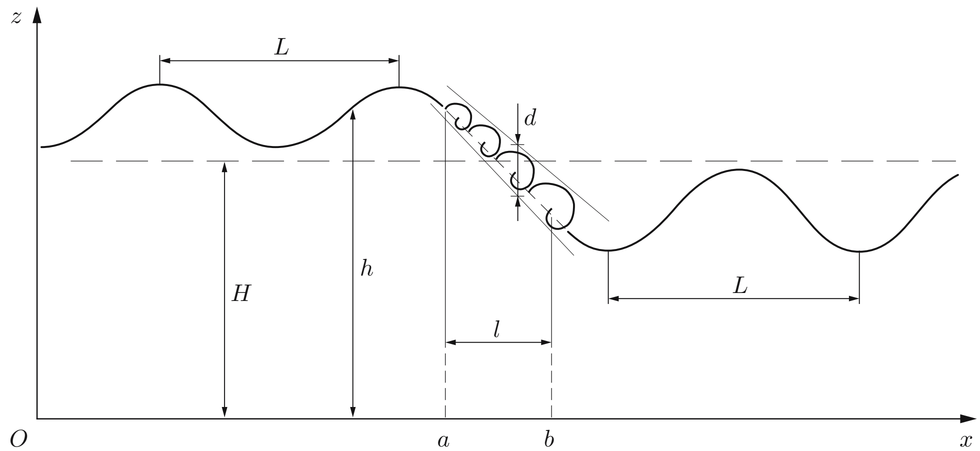

Fig. 2. Diagram of long-wave flow with a transition region of turbulent vortex flow modeled by a discontinuous wave.

3. Derivation of the Shallow Water Equations with Allowance for the Transition Region at the Discontinuous-Wave Front. Because in the first approximation of the shallow water equations, discontinuous solutions are discontinuous waves that model the transition regions

$$G = \{(x,t)\colon a(t) \le x \le b(t)\} \tag{3.1}$$

of turbulent vortex flow (Fig. 2), in view of the basic hypothesis of the long-wave approximation [1], the characteristic length $l = O(b(t) - a(t))$ of such transition regions should simultaneously satisfy the two inequalities $H \ll l \ll L$ (H is the characteristic flow depth and L is the characteristic wavelength in the region of $\overline{G} = \mathbb{R}^2 \setminus G$ of potential flow without discontinuous waves). Thus, the description of discontinuous waves as discontinuous solutions in the long-wave approximation of shallow water theory involves the following two successive passages to the limit:

$$\delta = H/l \to 0, \qquad \varepsilon = l/L \to 0.$$

We first consider the shallow water equations obtained from the spatially two-dimensional equations of fluid motion for

$$H \to 0, \quad l = \text{const}, \quad L = \text{const} \quad \Rightarrow \quad \delta \to 0.$$

For this, we assume that in the region $\overline{G}$, the flow is potential and is described by the continuity equation

$$u_x + w_z = 0, \tag{3.2}$$

the equation of no vortex

$$u_z - w_x = 0 \tag{3.3}$$

and the Euler equation

$$\boldsymbol{v}_t + (\boldsymbol{v}\nabla)\boldsymbol{v} + \nabla(p + gz) = 0, \tag{3.4}$$

which can be written in component form

$$u_t + uu_x + wu_z + p_x = 0; \tag{3.5}$$

$$w_t + uw_x + ww_z + p_z + g = 0. \tag{3.6}$$

Here $\nabla = (\partial/\partial x, \partial/\partial z)$ is the two-dimensional gradient operator, $\boldsymbol{v}(x,z,t) = (u,w)$ is the two-dimensional velocity, and $p(x,z,t)$ is the pressure divided by the constant fluid density.

Because the fluid flow occurs over a horizontal bottom which coincides with the x axis, for system (3.2)–(3.6) we impose the following natural boundary conditions [1]: at the bottom at $z = 0$, the nonpenetration condition

$$w(x,0,t) = 0, \tag{3.7}$$

and on the free surface at $z = h$ [$h = h(x,t)$ is the flow depth], the condition of constant pressure

$$p(x,h,t) = p_0 = 0 \tag{3.8}$$

and the kinematic condition

$$w(x,h,t) = h_t + u(x,h,t)h_x. \tag{3.9}$$

Writing Eqs. (3.2)–(3.6) and the boundary conditions (3.7)–(3.9) in the dimensionless variables

$$z^* = \frac{z}{H}, \quad h^* = \frac{h}{H}, \quad g^* = \frac{g}{a}, \quad u^* = \frac{u}{v}, \quad p^* = \frac{p}{v^2}; \tag{3.10}$$

$$x^* = \frac{x-\tilde{x}}{L}, \quad t^* = \frac{v(t-\tilde{t})}{L}, \quad w^* = \frac{Lw}{vH}, \quad \tilde{x} = \text{const}, \quad \tilde{t} = \text{const}, \tag{3.11}$$

where $v = \sqrt{aH}$ is the characteristic velocity and a is the characteristic acceleration, and introducing the small parameter $\Delta = H/L$, we obtain

$$\frac{\partial u^*}{\partial x^*} + \frac{\partial w^*}{\partial z^*} = 0, \qquad \frac{\partial u^*}{\partial z^*} - \Delta^2 \frac{\partial w^*}{\partial x^*} = 0; \tag{3.12}$$

$$\frac{\partial u^*}{\partial t^*} + u^* \frac{\partial u^*}{\partial x^*} + w^* \frac{\partial u^*}{\partial z^*} + \frac{\partial p^*}{\partial x^*} = 0; \tag{3.13}$$

$$\Delta^2 \Big(\frac{\partial w^*}{\partial t^*} + u^* \frac{\partial w^*}{\partial x^*} + w^* \frac{\partial w^*}{\partial z^*} \Big) + \frac{\partial p^*}{\partial z^*} + g^* = 0; \tag{3.14}$$

$$w^*(x^*, 0, t^*) = 0; \tag{3.15}$$

$$p^*(x^*, h^*, t^*) = 0; \tag{3.16}$$

$$w^*(x^*, h^*, t^*) = \frac{\partial h^*}{\partial t^*} + u^*(x^*, h^*, t^*) \frac{\partial h^*}{\partial x^*}. \tag{3.17}$$

If $\delta \to 0$, then, $\Delta = \delta\varepsilon \to 0$, and from the second equation (3.12), we obtain

$$\frac{\partial u^*}{\partial z^*} = 0 \quad \Rightarrow \quad u^* = u^*(x^*, t^*), \tag{3.18}$$

and from Eq. (3.14), in view of boundary condition (3.16), it follows that the fluid pressure varies under the hydrostatic law

$$p^* = g^*(h^* - z^*). \tag{3.19}$$

Integrating the first equation (3.12) with respect to z^* from 0 to h^* taking into account the integral identity

$$\int\limits_0^h \frac{\partial f}{\partial x}\, dz = \frac{\partial}{\partial x}\Big(\int\limits_0^h f\, dz \Big) - f\Big|_{z=h} \frac{\partial h}{\partial x}, \tag{3.20}$$

boundary conditions (3.15) and (3.17), and formulas (3.18), we obtain the mass conservation law

$$\frac{\partial h^*}{\partial t^*} + \frac{\partial q^*}{\partial x^*} = 0, \qquad q^* = h^* u^*. \tag{3.21}$$

Equations (3.13), in view of formulas (3.18) and (3.19), implies the law of conservation of the local momentum

$$\frac{\partial u^*}{\partial t^*} + \frac{\partial}{\partial x^*}\Big(\frac{(u^*)^2}{2} + g^* h^* \Big) = 0. \tag{3.22}$$

Combining Eq. (3.21) multiplied by u^* and Eq. (3.22) multiplied by h^*, we obtain the total momentum conservation law

$$\frac{\partial q^*}{\partial t^*} + \frac{\partial}{\partial x^*}\Big(q^* u^* + \frac{g^*(h^*)^2}{2} \Big) = 0. \tag{3.23}$$

As a result, for $\delta \to 0$ in the potential flow region $\overline{G}$, the classical system (3.21), (3.23) of irrotational shallow water is obtained, which coincides with the basic system (1.1), (1.2).

Remark 1. The above derivation of the shallow water equations (3.21) and (3.23) differs from the more standard method of their derivation first proposed in [26], according to which the dimensionless vertical velocity is defined by the formula

$$w^{**} = Hw/(vL) = \Delta^2 w^*,$$

which, in dimensionless variables (3.10), (3.11), preserves the form of the no-vortex equation

$$\frac{\partial u^*}{\partial z^*} - \frac{\partial w^{**}}{\partial x^*} = 0,$$

but leads to a change in the form of the continuity equation

$$\Delta^2 \frac{\partial u^*}{\partial x^*} + \frac{\partial w^*}{\partial z^*} = 0.$$

As a result, the shallow water equations (1.1) and (1.2) are obtained not for $\Delta = 0$ but only as a first approximation in the parameter Δ^2, which explains the origin of the term "the first approximation of shallow water theory" [1, 26].

An advantage of the dimensionless variables (3.10) and (3.11) is that their use allows one to derive the shallow water equations (3.21) and (3.23) even in the zero (or initial) approximation in the parameter Δ^2. In addition, as noted in [27], this method of specifying dimensionless quantities is more natural since it preserves the form of the kinematic relation for a moving particle $\boldsymbol{v} = d\boldsymbol{r}/dt$ in the dimensionless variables, and, in addition, it explicitly introduces the underlying hypothesis of hydrodynamic theory that, in the case of shallow water, the vertical acceleration of fluid particles is smaller than the acceleration due to gravity the.

4. Shallow Water Equations in the Transition Region $\boldsymbol{G}$. Since the flow is vortex and turbulent by virtue of the above assumptions in the transition region (3.1), it can be described using the spatially two-dimensional continuity equations (3.2) and the Navier–Stokes equations

$$\boldsymbol{v}_t + (\boldsymbol{v}\nabla)\boldsymbol{v} + \nabla(p + gz) = 2\,\mathrm{div}\,(\nu D), \tag{4.1}$$

where

$$D = \begin{pmatrix} u_x & (u_z + w_x)/2 \\ (u_z + w_x)/2 & w_z \end{pmatrix} \tag{4.2}$$

is the two-dimensional strain rate tensor, $\nu(\boldsymbol{v}) = \nu_1 + \nu_2(\boldsymbol{v})$ is the viscosity coefficient, which is equal to the sum of the kinematic viscosity $\nu_1 = \mathrm{const}$ and the turbulent viscosity $\nu_2(\boldsymbol{v})$. Since $\nu_2 \gg \nu_1$, ignoring the quantity ν_1, we assume that $\nu(\boldsymbol{v}) = \nu_2(\boldsymbol{v})$. In view of (4.2), Eq. (4.1) can be written in component form

$$u_t + uu_x + wu_z + p_x = 2(\nu u_x)_x + (\nu(u_z + w_x))_z; \tag{4.3}$$

$$w_t + uw_x + ww_z + p_z + g = (\nu(u_z + w_x))_x + 2(\nu w_z)_z. \tag{4.4}$$

For system (3.2), (4.3), (4.4), we impose boundary conditions. At the bottom at $z = 0$, we specify the non-penetration condition (3.7) for the vertical velocity w and the no-slip or slip condition for the horizontal component u [28]. On the free surface, we distinguish a strip S of the characteristic thickness d (see Fig. 2) inside which breaks leading to the formation of small-scale turbulent vortex structures occur. Assuming that $d \ll H$ and passing to the limit as $d \to 0$, we replace this strip by the smooth free-surface line

$$z - h(x, t) = 0, \tag{4.5}$$

on which the flow parameters are the flow parameters inside it averaged over the thickness of the strip S. This passage to the limit allows the flow to be described within the framework of Eqs. (3.2) and (4.1) specified inside the regular region

$$\tilde{G} = \{(x, z, t)\colon a(t) \le x \le b(t),\ 0 \le z \le h(x, t)\} \tag{4.6}$$

with the material free boundary (4.5), on which the following kinematic (3.9) and dynamic conditions are satisfied [28]:

$$p\boldsymbol{n} = 2(\nu D + \sigma N E)\boldsymbol{n} + \nabla_h \sigma. \tag{4.7}$$

Here E is the unit tensor, $\boldsymbol{n}$ is the unit outward normal vector to the free-surface line (4.5),

$$\boldsymbol{n} = (-h_x, 1)/r \qquad (r = \sqrt{1 + (h_x)^2}\,), \tag{4.8}$$

$N = (1/2)(h_x/r)_x$ is the average curvature of this line,

$$\nabla_h = \nabla - \boldsymbol{n}(\boldsymbol{n}\nabla) = \boldsymbol{s}(\boldsymbol{s}\nabla) \tag{4.9}$$

is the gradient operator along the line (4.5), and $\boldsymbol{s} = (1, h_x)/r$ is the unit vector tangent to the line (4.5). The function $\sigma = \sigma(\boldsymbol{v})$ specifies the free energy concentrated on the line (4.5). This energy is induced by turbulent vortex motion inside the strip S, which, for $d \to 0$, is pulled to the free surface line (4.5). Multiplying the condition (4.7) scalarly by the unit vectors $\boldsymbol{n}$ and $\boldsymbol{s}$ and taking into account that, by virtue of formulas (4.8) and (4.9), $\boldsymbol{n}\boldsymbol{s} = \boldsymbol{n}\nabla_h\sigma = 0$, we write this vector condition in the form of two scalar relations

$$p = 2(\nu\boldsymbol{n}D\boldsymbol{n} + \sigma N), \qquad 2\nu\boldsymbol{s}D\boldsymbol{n} + \boldsymbol{s}\nabla\sigma = 0, \tag{4.10}$$

where

$$r^2\boldsymbol{n}D\boldsymbol{n} = w_z - (u_z + w_x)h_x - u_x h_x^2, \qquad r^2\boldsymbol{s}D\boldsymbol{n} = (u_z + w_x)(1 - h_x^2)/2 - (u_x - w_z)h_x,$$

$$r\boldsymbol{s}\nabla\sigma = \frac{d\sigma(\boldsymbol{v})}{dx} = \sigma_u(u_x + u_z h_x) + \sigma_w(w_x + w_z h_x).$$

In Eqs. (3.2), (4.3), and (4.4) and boundary conditions (3.7), (3.9), and (4.10), we convert to the dimensionless variables (3.10) and

$$x_* = \frac{x - \tilde{x}}{l}, \quad t_* = \frac{v(t - \tilde{t})}{l}, \quad w_* = \frac{lw}{vH}, \quad \nu_* = \frac{l\nu}{vH^2}, \quad \sigma_* = \frac{\sigma}{Hv^2}. \tag{4.11}$$

As a result, the equations are written as

$$\frac{\partial u^*}{\partial x_*} + \frac{\partial w_*}{\partial z^*} = 0; \tag{4.12}$$

$$\frac{\partial u^*}{\partial t_*} + u^*\frac{\partial u^*}{\partial x_*} + w_*\frac{\partial u^*}{\partial z^*} + \frac{\partial p^*}{\partial x_*} = 2\delta^2\frac{\partial}{\partial x_*}\Big(\nu_*\frac{\partial u^*}{\partial x_*}\Big) + \frac{\partial}{\partial z^*}\Big(\nu_*\Big(\frac{\partial u^*}{\partial z^*} + \delta^2\frac{\partial w_*}{\partial x_*}\Big)\Big); \tag{4.13}$$

$$\delta^2\Big(\frac{\partial w_*}{\partial t_*} + u^*\frac{\partial w_*}{\partial x_*} + w_*\frac{\partial w_*}{\partial z^*}\Big) + \frac{\partial p^*}{\partial z^*} + g^* = \delta^2\frac{\partial}{\partial x_*}\Big(\nu_*\Big(\frac{\partial u^*}{\partial z^*} + \delta^2\frac{\partial w_*}{\partial x_*}\Big)\Big) + 2\delta^2\frac{\partial}{\partial z^*}\Big(\nu_*\frac{\partial u^*}{\partial x_*}\Big), \tag{4.14}$$

and the boundary conditions become

$$w_*(x_*, 0, t_*) = 0; \tag{4.15}$$

$$w_*(x_*, h^*, t_*) = \frac{\partial h^*}{\partial t_*} + u^*(x_*, h^*, t_*)\,\frac{\partial h^*}{\partial x_*}; \tag{4.16}$$

$$p^* = 2\delta^2(\nu_*(\boldsymbol{n}D\boldsymbol{n})_* + \sigma_* N_*), \qquad 2r\nu_*(\boldsymbol{s}D\boldsymbol{n})_* + \frac{d\sigma_*(u^*, w_*)}{dx_*} = 0, \tag{4.17}$$

where

$$r^2(\boldsymbol{n}D\boldsymbol{n})_* = \frac{\partial w_*}{\partial z^*} - \Big(\frac{\partial u^*}{\partial z^*} + \delta^2\,\frac{\partial w_*}{\partial x_*}\Big)\frac{\partial h^*}{\partial x_*} - \delta^2\,\frac{\partial u^*}{\partial x_*}\Big(\frac{\partial h^*}{\partial x_*}\Big)^2,$$

$$r^2(\boldsymbol{s}D\boldsymbol{n})_* = \frac{1}{2}\Big(\frac{\partial u^*}{\partial z^*} + \delta^2\,\frac{\partial w_*}{\partial x_*}\Big)\Big(1 - \delta^2\Big(\frac{\partial w_*}{\partial x_*}\Big)^2\Big) - \delta^2\,\frac{\partial h^*}{\partial x_*}\Big(\frac{\partial u^*}{\partial x_*} - \frac{\partial w_*}{\partial z^*}\Big),$$

$$N_* = \frac{1}{2}\,\frac{\partial}{\partial x_*}\Big(\frac{1}{r}\,\frac{\partial h^*}{\partial x_*}\Big), \qquad r = \sqrt{1 + \delta^2\Big(\frac{\partial h^*}{\partial x_*}\Big)^2}.$$

In passing to the limit as $\delta \to 0$, in view of the first boundary condition (4.17), which becomes

$$p^*(x_*, h^*, t_*) = 0,$$

it follows from Eq. (4.14) that the pressure in the region (4.6) varies under the hydrostatic law (3.19), and, using (3.19), from Eq. (4.13) we obtain

$$\frac{\partial u^*}{\partial t_*} + u^* \frac{\partial u^*}{\partial x_*} + w_* \frac{\partial u^*}{\partial z^*} + g^* \frac{\partial h^*}{\partial x_*} = \frac{\partial}{\partial z^*}\Big(\nu_* \frac{\partial u^*}{\partial z^*}\Big). \tag{4.18}$$

The second boundary condition (4.17) for $\delta \to 0$ becomes

$$\nu_* \frac{\partial u^*}{\partial z^*}\Big|_{z^*=h^*} + \frac{d\sigma_*(u^*, w_*)}{dx_*} = 0. \tag{4.19}$$

Integrating Eq. (4.12) with respect to z^* from 0 to h^*, in view of formulas (3.20) and boundary conditions (4.15) and (4.16), we obtain the mass conservation law

$$\frac{\partial h^*}{\partial t_*} + \frac{\partial q^*}{\partial x_*} = 0, \qquad q^* = \int\limits_0^{h^*} u^*(x_*, z^*)\, dz^* \tag{4.20}$$

in transition region (4.6).

For the specified functions $\nu(\boldsymbol{v})$ and $\sigma(\boldsymbol{v})$ [the first of them is specified in the region (4.6), and the second on the free surface (4.5)], Eqs. (4.12), (4.18), and (4.20) with the corresponding boundary conditions form a closed system of vortex shallow water equations which describe turbulent vortex flow (turbulent bore [3]) in the transition region (4.6). The other methods for describing the structure of a turbulent bore (in particular, using multilayered nonvortex shallow water models) were considered in [3, 29–32]. For $\nu = \sigma = 0$, system (4.12), (4.18), (4.20) becomes the ideal vortex shallow water equations, which were studied in [3, 33–37].

5. Total-Momentum Conservation Law in the Transition Region *G*. Combining Eq. (4.18) and Eq. (4.20) multiplied by u^*, we obtain the following equation in divergent form

$$\frac{\partial u^*}{\partial t_*} + \frac{\partial}{\partial x_*}\Big((u^*)^2 + g^* h^*\Big) + \frac{\partial}{\partial z^*}(u^* w_*) = \frac{\partial}{\partial z^*}\Big(\nu_* \frac{\partial u^*}{\partial z^*}\Big).$$

Integration of the above equation with respect to z^* from 0 to h^* taking into account Eq. (3.20), the formula

$$\int\limits_0^h \frac{\partial f}{\partial t}\, dz = \frac{\partial}{\partial t}\Big(\int\limits_0^h f\, dz\Big) - f\Big|_{z=h} \frac{\partial h}{\partial t},$$

and boundary conditions (4.15) and (4.16) leads to the total-momentum conservation law

$$\frac{\partial q^*}{\partial t_*} + \frac{\partial}{\partial x_*}\Big(\int\limits_0^{h^*} (u^*)^2 dz^* + \frac{g^*(h^*)^2}{2}\Big) = \nu_* \frac{\partial u^*}{\partial z^*}\Big|_{z^*=0}^{z^*=h^*} \tag{5.1}$$

in the transition region (3.1).

The quantity

$$R_b = -\nu_* \frac{\partial u^*}{\partial z^*}\Big|_{z^*=0} \tag{5.2}$$

on the right side of Eq. (5.1) is the bottom friction force, whose calculation requires the use of the boundary conditions at $z^* = 0$, leading to the formation of a near-bottom boundary layer. Since the irrotational shallow water equations (3.21) and (3.23), which are valid for the external region $\overline{G}$, ignore the bottom friction, in the conservation laws for vortex shallow water (4.20) and (5.1) specified in the transition region G, we will also ignore the bottom friction force (5.2) and the thickness of the near-bottom boundary layer. This allows the total-momentum conservation law (5.1) in the transition region G to be written as

$$\frac{\partial q^*}{\partial t_*} + \frac{\partial}{\partial x_*}\Big(\int\limits_0^{h^*} (u^*)^2 dz^* + \frac{g^*(h^*)^2}{2}\Big) = R, \tag{5.3}$$

where, in view of boundary condition (4.19), the quantity

$$R = \nu_* \frac{\partial u^*}{\partial z^*}\Big|_{z^*=h^*} = -\frac{d\sigma_*(u^*, w_*)}{dx_*}$$

characterizes the total-momentum losses due to the action of the free energy σ_* concentrated on the free surface.

For an approximate determination of the quantity R, we assume that, on the free surface (4.5) for $\delta \to 0$, the turbulent viscosity coefficient $\tilde{\nu} = \nu_*|_{z^*=h^*}$ and the vertical velocity component $\tilde{w} = w_*|_{z^*=h^*}$ are linked by the relation

$$\tilde{\nu} = \gamma^* \tilde{w} + o(\gamma^*), \qquad 0 < \gamma^* = \text{const} \ll 1. \tag{5.4}$$

The inequality $\gamma^* > 0$ follows from the inequalities $\tilde{\nu} > 0$ and $\tilde{w} > 0$, the last of which follows from the stability condition for discontinuous waves [5].

Remark 2. Formula (5.4) can be derived as follows. Assuming that the viscosity coefficient $\tilde{\nu}$ is a function of only the vertical velocity component $\tilde{w}$ to within $o(\delta)$, we expand this function in a Taylor series for $\tilde{w} = 0$ to within $O(\tilde{w}^{\,2})$. As a result, we have

$$\tilde{\nu}(\tilde{w}) = \tilde{\nu}(0) + \tilde{\nu}'(0)\tilde{w} + \tilde{\nu}''(\eta)\tilde{w}^2/2, \tag{5.5}$$

where $\eta \in (0, \tilde{w})$. Relation (5.4) follows from formula (5.5) provided that

$$\tilde{\nu}(0) = 0, \qquad \tilde{w}\,|\tilde{\nu}''(\eta)| \ll \tilde{\nu}'(0) \ll 1.$$

In this case, the parameter γ^* is defined by the formula

$$\gamma^* = \tilde{\nu}'(0).$$

In view of condition (5.4), Eq. (4.18) implies that, to within $o(\gamma^*)$,

$$R = \nu_* \frac{\partial u^*}{\partial z^*}\Big|_{z^*=h^*} = -\gamma^* \Big\{ \frac{\partial u^*}{\partial t_*} + \frac{\partial}{\partial x_*}\Big(\frac{(u^*)^2}{2} + g^* h^* \Big) \Big\}.$$

This allows the total-momentum conservation law (5.3) to be written in divergent form

$$\frac{\partial\,(q^* + \gamma^* u^*)}{\partial t_*} + \frac{\partial}{\partial x_*}\Big(\int\limits_0^{h^*} (u^*)^2 \, dz^* + \frac{g^*(h^*)^2}{2} + \gamma^* \Big(\frac{(u^*)^2}{2} + g^* h^* \Big) \Big) = 0. \tag{5.6}$$

In Sec. 6, Eq. (5.6) is used to derive a modified Hugoniot condition at the discontinuous-wave front for the total-momentum conservation law.

6. Modified Hugoniot Conditions at the Discontinuous-Wave Front. By passing to the limit

$$l \to 0, \qquad L = \text{const} \quad \Rightarrow \quad \varepsilon = l/L \to 0, \tag{6.1}$$

we obtain modified Hugoniot conditions at the discontinuous-wave front for the shallow water equations. If this passage to the limit is considered with respect to the external dimensionless variables (3.11), the internal region (3.1) is transformed to the discontinuity line

$$x^* = x^*(t^*) = \lim_{l \to 0} a^*(t^*) = \lim_{l \to 0} b^*(t^*) \qquad (a^* = a/L; \quad b^* = b/L) \tag{6.2}$$

for which we assume that

$$D^* = \frac{dx^*}{dt^*} = \lim_{l \to 0} \frac{da^*}{dt^*} = \lim_{l \to 0} \frac{db^*}{dt^*}. \tag{6.3}$$

Outside the discontinuity line (6.2), the flow is described by the smooth solution $\boldsymbol{u}^*(x^*, t^*) = (h^*, u^*)$ of Eqs. (3.21) and (3.22), which on both sides of this line takes the limiting values

$$\boldsymbol{u}_0^*(t^*) = \boldsymbol{u}^*(x^*(t^*) + 0, t^*), \qquad \boldsymbol{u}_1^*(t^*) = \boldsymbol{u}^*(x^*(t^*) - 0, t^*). \tag{6.4}$$

To obtain modified Hugoniot conditions relating the quantities (6.4), we fix the time $t^* = \tau$ and consider the passage to the limit (6.1) with respect to the internal dimensionless variables (4.11), where

$$\tilde{x} = Lx^*(\tau), \qquad \tilde{t} = \tau L/v. \tag{6.5}$$

In the dimensionless variables (4.11) and (6.5), the point with the coordinates $x^* = x^*(\tau)$ and $t^* = \tau$ on the discontinuity line (6.2) coincides with the coordinate origin $x_* = t_* = 0$.

Because formulas (3.11) and (4.11) imply that

$$dx^* = \varepsilon\, dx_*, \quad dt^* = \varepsilon\, dt_* \quad \Rightarrow \quad D^* = \frac{dx^*}{dt^*} = \frac{dx_*}{dt_*} = D_*,$$

taking into account that the derivative dD^*/dt^* does not depend on l, we obtain

$$\lim_{l\to 0} \frac{dD_*}{dt_*} = \lim_{l\to 0} \frac{dD^*}{dt_*} = \frac{dD^*}{dt^*} \lim_{l\to 0} \varepsilon = 0.$$

In view of formulas (6.2) and (6.3), this implies that, as $l \to 0$ ($\varepsilon \to 0$), the transition region (3.1) in the internal variables (4.11) and (6.5) is transformed to the strip of constant width

$$G_* = \{(x_*, t_*)\colon \xi_0 - D^* t_* \le x_* \le \xi_1 - D^* t_*\}, \tag{6.6}$$

where

$$\xi_0 = \lim_{l\to 0} a_*(0), \qquad \xi_1 = \lim_{l\to 0} b_*(0), \qquad D^* = D^*(\tau) = D_*(0), \qquad a_* = (a - \tilde{x})/l, \qquad b_* = (b - \tilde{x})/l.$$

On both sides of the strip G_*, by virtue of conditions (6.4) and the equalities

$$\frac{\partial u^*}{\partial x_*} = \varepsilon \frac{\partial u^*}{\partial x^*}, \qquad \frac{\partial u^*}{\partial t_*} = \varepsilon \frac{\partial u^*}{\partial t^*},$$

the solution is constant and is defined by the formula

$$\boldsymbol{u}^*(x_*, t_*) = \begin{cases} \boldsymbol{u}_0^*, & x_* \ge \xi_1 - D^* t_*, \\ \boldsymbol{u}_1^*, & x_* \le \xi_0 - D^* t_*, \end{cases} \tag{6.7}$$

where $\boldsymbol{u}_i^* = (h_i^*, u_i^*) = \boldsymbol{u}_i^*(\tau) = (h_i^*(\tau), u_i^*(\tau))$ $(i = 0, 1)$.

Thus, by passage to the limit (6.1) with respect to the internal dimensionless variables (4.11) and (6.5), the flow is described by Eqs. (4.12), (4.20), and (5.6) inside the strip (6.6), on whose boundary conditions (6.7) are satisfied. This problem admits a self-similar solution that depends on the variables $\xi = x_* - D^* t_*$ and z^*. We write Eqs. (4.20) and (5.6) in the variables ξ and z^* and integrate them with respect to ξ from ξ_0 to ξ_1 taking into account the following boundary conditions implied by formula (6.7):

$$h^*(\xi) = \begin{cases} h_0^*, & \xi \ge \xi_1, \\ h_1^*, & \xi \le \xi_0, \end{cases} \qquad u^*(\xi, z^*) = \begin{cases} u_0^*, & \xi \ge \xi_1, \\ u_1^*, & \xi \le \xi_0. \end{cases}$$

As a result, Eq. (4.20) leads to the standard Hugoniot condition

$$D^*[h^*] = [q^*] \tag{6.8}$$

for the mass conservation law (3.21), and Eq. (5.6) implies the relation

$$D^*[q^* + \gamma^* u^*] = [q^* u^* + g^*(h^*)^2/2 + \gamma^*((u^*)^2/2 + g^* h^*)]. \tag{6.9}$$

Returning to the dimensional variables by formulas (3.10), from relations (6.8) we obtain the standard Hugoniot condition (1.3) for the mass conservation law (1.1), and from relation (6.9), we have the modified Hugoniot condition

$$D[q + \gamma u] = [qu + gh^2/2 + \gamma(u^2/2 + gh)] \qquad (D = vD^*;\ \gamma = H\gamma^*) \tag{6.10}$$

for the total-momentum conservation law.

7. Modified Equations of Irrotational Shallow Water. Because the total-momentum losses due to the formation of small-scale turbulent vortex structures in the fluid surface layer occur only at discontinuous-wave fronts, it follows that, on the continuous solutions, the modified irrotational shallow water equations taking into account these losses should be equivalent to the classical equations (1.1) and (1.2) and on the discontinuity lines, they should imply the Hugoniot conditions (1.3) and (6.10). These requirements are satisfied by the system consisting of the basic mass conservation law (1.1) and the modified total-momentum conservation law

$$(q + \gamma u)_t + (qu + gh^2/2 + \gamma(u^2/2 + gh))_x = 0. \tag{7.1}$$

Equation (7.1) is a linear combination of Eqs. (1.2) and (2.7). Using the notation $Q = q + \gamma u = \bar{h}u$, $\bar{h} = h + \gamma$, $\tilde{h} = h + \gamma/2$, and $\hat{h} = h + 2\gamma$, Eq. (7.1) can be written in more compact form

$$Q_t + (\tilde{h}u^2 + gh\hat{h}/2)_x = 0, \tag{7.2}$$

and the corresponding Hugoniot condition in the form

$$D[Q] = [\tilde{h}u^2 + gh\hat{h}/2]. \tag{7.3}$$

Since for the transformation $\boldsymbol{Q} = \boldsymbol{Q}(\boldsymbol{q})$, in which $\boldsymbol{q} = (h, q)$ and $\boldsymbol{Q} = (h, Q)$ and which transforms system (1.1), (1.2) to system (1.1), (7.2), the Jacobi matrix determinant has the form

$$\left|\frac{\partial \boldsymbol{Q}}{\partial \boldsymbol{q}}\right| = \begin{vmatrix} 1 & 0 \\ -\gamma u/h & 1 + \gamma/h \end{vmatrix} = 1 + \frac{\gamma}{h};$$

on the smooth solutions, these systems are equivalent for all $h \neq 0$, i.e., over the entire hyperbolicity region ($h > 0$) of the shallow water model. To analyze the compatibility of systems (1.1), (1.2) and (1.1), (7.2) on discontinuous solutions, we transform relation (7.3). Using notation (1.5), condition (1.3) and formulas (1.6) and (1.7), relation (7.3) can be written as

$$(h_0 h_1 + \gamma\langle h\rangle)[u]^2/[h] = g(\langle h\rangle + \gamma)[h],$$

which implies the dependence

$$[u] = B_2(h_0, h_1, \gamma^*)[h], \tag{7.4}$$

where

$$B_2(h_0, h_1, \gamma^*) = \sqrt{g(\langle h\rangle + \gamma)/(h_0 h_1 + \gamma\langle h\rangle)}, \qquad \gamma = H\gamma^*. \tag{7.5}$$

Because, in view of formula (1.9),

$$B_1^2 - B_2^2 = \frac{g\langle h\rangle}{h_0 h_1} - \frac{g(\langle h\rangle + \gamma)}{h_0 h_1 + \gamma\langle h\rangle} = \frac{\gamma g[h]^2}{h_0 h_1 (h_0 h_1 + \gamma\langle h\rangle)}, \tag{7.6}$$

dependences (1.8) and (7.4) are different for all $[h] = h_1 - h_0 \neq 0$. This implies that systems of conservation laws (1.1), (1.2) and (1.1), (7.2) are incompatible on discontinuous waves of any finite amplitude $[h] \neq 0$. At the same time, formula (7.6) implies that function (7.5) can be expanded in the small parameter γ^*

$$B_2(h_0, h_1, \gamma^*) = B_1(h_0, h_1)(1 + [h^*]^2\gamma^*/(h_0^* h_1^* \langle h^*\rangle) + O((\gamma^*)^2))$$

by virtue of which, for finite dimensionless depths h_0^* and h_1^*, condition (7.4) differs from the classical condition (1.8) only by a quantity of order $O(\gamma^*[h^*]^2)$. Moreover, in contrast to the classical condition (1.8), the modified condition (7.4) at $h_0 \to 0$ becomes the finite relation

$$u_1 = \sqrt{gh_1(h_1 + 2\gamma)/\gamma} = \sqrt{\theta g h_1}, \tag{7.7}$$

where

$$\theta = u_1^2/(gh_1)^2 = 2 + h_1/\gamma = 2 + h_1^*/\gamma^* \tag{7.8}$$

is the Froude number behind the front of a discontinuous wave propagating over a dry bed.

Thus, in contrast to the classical system (1.1), (1.2), the modified system of conservation laws of shallow water theory (1.1), (7.2) admits discontinuous wave propagation over a dry bed $h_0 = 0$, and for finite dimensionless depths $h_0^* > 0$ and $h_1^* > 0$, its corresponding Hugoniot conditions (1.3) and (7.3) coincide with the classical conditions (1.3), (1.4) to within $O(\gamma^*[h^*]^2)$.

8. Stable Discontinuous Waves Admitted by the Modified Shallow Water Equations. We distinguish stable discontinuous waves admitted by the basic conservation law of mass (1.1) and the modified conservation law of total momentum (7.2). If a discontinuous wave propagates over the dry bed (2.1), (2.2), this problem, in essence, was solved in Sec. 3 where it was shown that this wave is stable under condition (2.11) when it flows on the dry bed, and it is unstable under condition (2.12) when it runs off the dry bed. In the present section, we consider the general case of discontinuous-wave propagation over a bed of finite depth.

In a coordinate system in which the discontinuous-wave velocity $D = 0$, from the Hugoniot condition (1.3) we obtain

$$q_1 = q_0 = q, \tag{8.1}$$

and from relation (7.4), in view of (8.1), we find

$$q^2 = \frac{B_2^2[h]^2}{[h^{-1}]^2} = \frac{g(\langle h\rangle + \gamma)h_0^2 h_1^2}{h_0 h_1 + \gamma\langle h\rangle}. \tag{8.2}$$

Setting

$$h_1 > h_0 > 0, \tag{8.3}$$

we show that, ahead of a standing jump, the flow (8.1), (8.2) is supercritical, i.e., satisfies the inequality

$$v_0^2 = \frac{q^2}{h_0^2} = \frac{g(\langle h\rangle + \gamma)h_1^2}{h_0 h_1 + \gamma\langle h\rangle} > c_0^2 = gh_0, \tag{8.4}$$

and behind the jump, it is subcritical, i.e., satisfies the inequality

$$v_1^2 = \frac{q^2}{h_1^2} = \frac{g(\langle h\rangle + \gamma)h_0^2}{h_0 h_1 + \gamma\langle h\rangle} < c_1^2 = gh_1. \tag{8.5}$$

Since inequality (8.4) can be written as

$$h_1(h_1\langle h\rangle - h_0^2) + \gamma(h_1^2 - \langle h\rangle h_0) > 0,$$

and inequality (8.5) can be written as

$$h_0(h_1^2 - \langle h\rangle h_0) + \gamma(h_1\langle h\rangle - h_0^2) > 0,$$

their validity, in view of condition (8.3), follows from the obvious inequalities $h_1 > \langle h\rangle = (h_0 + h_1)/2 > h_0$.

Inequalities (8.4) and (8.5) imply that the standing jump (8.1)–(8.3) satisfies the characteristic stability criterion (2.13) for $q < 0$ and does not satisfy it for $q > 0$. This implies that, in a coordinate system in which the wave front velocity $D = 0$, the stable discontinuous waves admitted by the modified shallow water equations (1.1) and (7.2) are distinguished by the condition

$$q[h] = q(h_1 - h_0) < 0, \tag{8.6}$$

which implies that the flow depth increases as the fluid passes through the discontinuity. In transforming to a coordinate system in which the fluid in the region with a smaller depth is at rest, from inequalities (8.6) we find that the stable discontinuity waves propagating over a stationary background $u_0 = 0$ are distinguished by the condition

$$D[h] = D(h_1 - h_0) > 0, \tag{8.7}$$

which generalizes conditions (2.1) and (2.11).

Let us use the energetic stability criterion for discontinuous waves [5], according to which the total flow energy decreases in passing through a discontinuity. Relation (2.9) implies that in a coordinate system in which $D = 0$, the total-energy loss condition at a discontinuous-wave front is given by the inequality

$$[2ue + ghq] = [q(v^2 + 2gh)] > 0.$$

Transforming this inequality with the use of formulas (8.1) and (8.2), we obtain the condition

$$q(q^2[h^{-2}] + 2g[h]) = 2q[h]\Big(g - \frac{\langle h\rangle q^2}{h_0^2 h_1^2}\Big) = -\frac{gq[h]^3}{2(h_0 h_1 + \gamma\langle h\rangle)} > 0,$$

which is equivalent to condition (8.6).

Thus, as in the case of the classical system (1.1), (1.2) in the case of the modified system (1.1), (7.2), the characteristic and energetic stability criteria for discontinuous waves are equivalent, and the stable discontinuities distinguished by these criteria are specified by the same inequalities (8.6) and (8.7) as in the classical case [5].

9. Dam-Break Problem with a Dry Bed in the Tailwater. As an example, we consider the water wave flows resulting from dam break in a rectangular bed with a horizontal bottom and a dry bed in the tailwater.

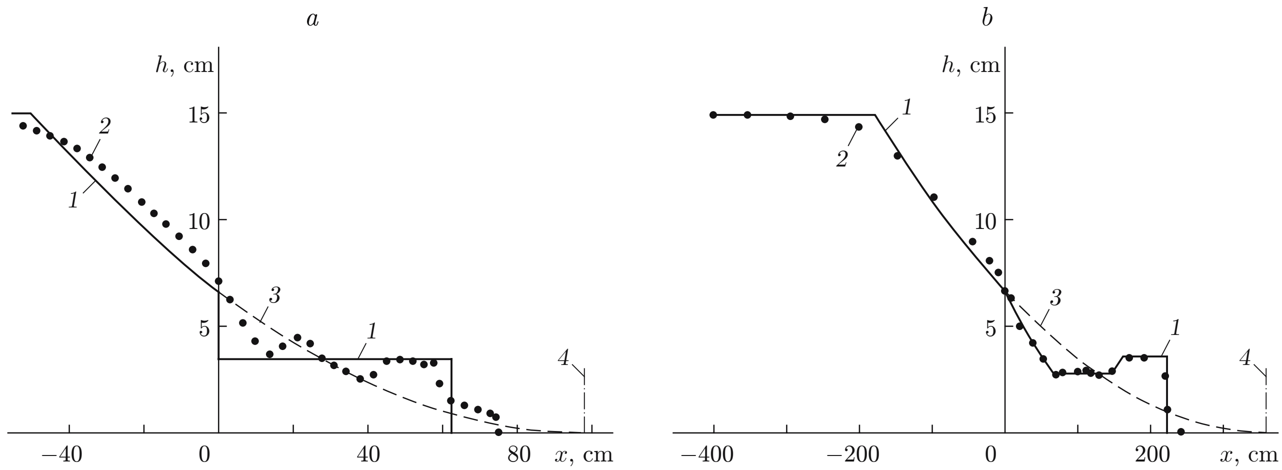

Fig. 3. Wave profile in the dam-break problem with a dry bed in the tailwater for $t = 0.41$ (a) and 1.47 sec (b); curves 1 refer to calculation results and curves 2 refer to experimental data; curves 3 are the classical depression wave profiles in the tailwater; the right boundary of the classical depression wave is marked as 4.

The points in Fig. 3 show the water free surface profiles at the times $t = 0.41$ (a) and 1.47 sec (b) obtained in laboratory modeling of flow in a rectangular tank. This wave flow arose from a sudden removal (at $t = 0$) of the flat shield located at the point $x = 0$, which bounded the stationary fluid of depth $H_0 = 15$ cm in the headwater at $x < 0$ (a detailed description of the results of the experiment is given in [21]).

In shallow water theory, this problem is formulated as the Cauchy problem of discontinuity decay with the following piecewise-constant initial data:

$$h(x,0) = \begin{cases} H_0, & x \le 0, \\ 0, & x > 0, \end{cases} \qquad u(x,0) = 0. \tag{9.1}$$

The exact solution of this problem obtained using the classical basic conservation laws of mass (2.1) and total momentum (2.2) is a centered depression r-wave, in which the flow parameters are defined by the formulas [1, 5]

$$h(x,t) = (2c_0 - \xi)^2/(9g), \quad u(x,t) = (2/3)(c_0 + \xi), \quad -c_0 \le \xi = x/t \le 2c_0 \tag{9.2}$$

($c_0 = \sqrt{gH_0}$ is the initial velocity of propagation of small perturbations in the headwater). In Fg. 3, the solid curve which at $x < 0$ becomes the dashed curve corresponds to solution (9.2) at $x > 0$. From Fig. 3 it follows that the depression wave (9.2) provides a good fit to the results of the experiment in the headwater (especially at the time $t = 1.47$ sec) and a much worse fit in the tailwater. Therefore, we modify the exact solution (9.2) only in the tailwater, i.e., at $x > 0$.

The steep head part of the experimental wave, whose front undergoes periodic breaks and whose propagation velocity is much lower than the velocity of motion of the right boundary of the depression wave (9.2), will be modeled by the discontinuous wave (2.2), (7.7) propagating over a dry bed (2.1.) In view of this, the exact solution of problem (9.1) can be constructed as a discontinuous wave of the form (2.2), (7.7), which is conjugate through the constant flow region (h_A, u_A) with the left part of the depression wave (9.2). In Fig. 4, this solution is shown by the solid curve $h^* A_1 A_2 x_5$. The constant-flow parameters (h_A and u_A) are found using the method of adiabats [5] as the coordinates of the point of intersection of the monotonically decreasing wave r adiabat

$$u = 2\sqrt{g}\,(\sqrt{H_0} - \sqrt{h}\,) \qquad (h < H_0) \tag{9.3}$$

and the monotonically increasing nonclassical shock s-adiabat

$$u = \sqrt{\theta g h}, \tag{9.4}$$

whose equation follows from formula (7.7). Solution of the system (9.3), (9.4) yields

$$h_A = \alpha^2 H_0, \qquad u_A = D_A = \alpha\sqrt{\theta g H_0}, \qquad \alpha = 2/(2 + \sqrt{\theta}).$$

The dashed curve in Fig. 4 shows the continuation of the depression wave (9.2) to the right of the point A_1.

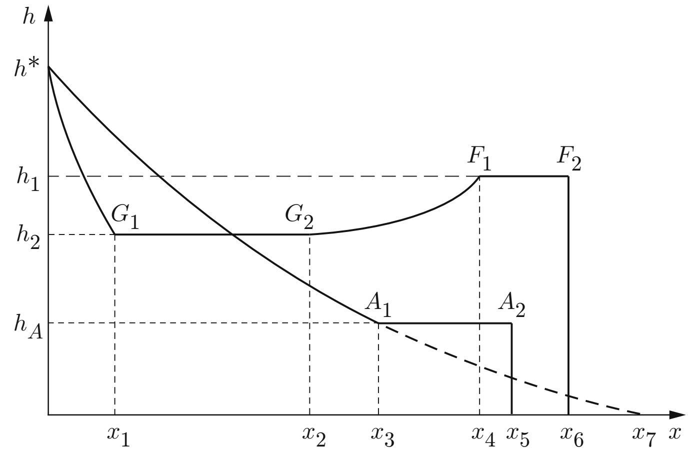

Fig. 4. Wave profiles obtained in modeling of the dam-break problem with a dry bed in the tailwater.

From a comparison of Figs. 3 and 4, it follows that the exact solution of problem (9.1), shown in Fig. 4 by the curve $h^*A_1A_2x_5$, correctly reproduces the steep profile of the experimental wave head but does not reflect the fact that, on the left side of the tailwater, the experimental points are considerably lower than the depression wave level (9.2). The reason for this is that the given solution ignores the strong vertical flow resulting from the breaking of the vertical water wall immediately after the removal of the shield.

Within the framework of the vertically averaged shallow water equations, the only possible method of locally accounting for the strong vertical flows comparable with the horizontal flows is to introduce discontinuities of the flow parameters, i.e., discontinuities of the depths and horizontal velocities [23]. From the results of the experiments it follows that, after the removal of the shield, the flow parameters at the initial discontinuity point $x = 0$ rapidly reach the critical values $h^* = h(0,t) = 4H_0/9$ and $u^* = u(0,t) = 2c_0/3$ and then remain almost constant throughout the experiment. This allows the initial vertical flow to be taken into account by using the simplified approach proposed in [23], in which the initial depth discontinuity $[0, H_0]$ is instantaneously transformed to a standing jump $[h_1, h^*]$. Here h_1 is the depth in the constant-flow zone (h_1, u_1) between the jump $[h_1, h^*]$ located at the point $x = 0$ and the discontinuous wave propagating at a constant velocity over the dry bed.

The Hugoniot condition (1.3) for the mass conservation law (1.1) implies that, for a stationary jump $[h_1, h^*]$, the flow rate is constant:

$$[q] = 0 \quad \Rightarrow \quad q^* = h^*u^* = q_1 = h_1u_1; \tag{9.5}$$

therefore, the supercritical flow parameters (h_1, u_1) are defined as the coordinates of the point at which the shock adiabat (9.4) intersects the hyperbola

$$u = q^*/h, \qquad q^* = h^*u^* = 8H_0c_0/27. \tag{9.6}$$

From system (9.5), (9.6), we obtain

$$h_1 = \sqrt[3]{(q^*)^2/(\theta g)}, \qquad u_1 = \sqrt[3]{\theta g q^*}. \tag{9.7}$$

In Fig. 3a, the profile of the self-similar solution constructed is shown by solid curve 1, and in Fig. 4, it is shown by the curve $h^*h_1F_1F_2x_6$. At $x > 0$, in this solution there is, in essence, an artificial separation between the vertical and horizontal real flows in the tailwater. The vertical flows are concentrated at the depth jump $[h_1, h^*]$ at the point $x = 0 + 0$, and the horizontal are distributed in the constant-flow zone h_1F_2 behind the discontinuous-wave front (see Fig. 4). This description of the initial stage of the tailwater flow is in good agreement with the experimental results presented in [22].

The discontinuity $[h_1, h^*]$ is unstable, and the time of its existence t_1 is defined as the characteristic time during which the vertical velocities at the dam location are comparable with the horizontal velocities. The value of t_1 is calculated from the formula $t_1 = \tau\sqrt{H_0/g}$, where τ is the dimensionless time parameter determined by matching to the results of laboratory experiments. At the time t_1, the discontinuity $[h_1, h^*]$ decays, which, in shallow water theory, is formulated as the discontinuity decay problem

$$h(x,t_1) = \begin{cases} h^*, & x \le 0, \\ h_1, & x > 0, \end{cases} \qquad u(x,t_1) = \begin{cases} u^*, & x \le 0, \\ u_1, & x > 0, \end{cases} \tag{9.8}$$

whose solution, shown by the curve $h^*G_1G_2F_1$ in Fig. 4, consists of two centered depression waves connected by a constant-flow region (h_2, u_2). The quantities h_2 and u_2 are found as the coordinates of the point of intersection of the monotonically decreasing r-adiabat (9.3) and the monotonically increasing s-adiabat:

$$u = u_1 - 2\sqrt{g}\,(\sqrt{h_1} - \sqrt{h}\,), \qquad h < h_1. \tag{9.9}$$

From system (9.3), (9.9), we obtain

$$h_2 = ((c_0 + c_1)/2 - u_1/4)/g, \qquad u_2 = c_0 - c_1 + u_1/2, \tag{9.10}$$

where $c_0 = \sqrt{gH_0}$ and $c_1 = \sqrt{gh_1}$. In the depression r-wave, shown by the curve h^*G_1 in Fig. 4, the flow parameters are calculated from the formulas

$$h(x,t) = (2c_0 - \eta)^2/(9g), \qquad u(x,t) = 2(c_0 + \eta)/3, \qquad 0 \le \eta \le u_2 - c_2, \tag{9.11}$$

and in the depression s-wave, shown by the curve G_2F_1 in Fig. 4, they are calculated from the formulas

$$h(x,t) = (\eta + 2c_1 - u_1)^2/(9g), \qquad u(x,t) = (2\eta + v_1 - 2c_1)/3, \tag{9.12}$$

where $u_2 + c_2 \le \eta \le u_1 + c_1$, $c_2 = \sqrt{gh_2}$, and $\eta = x/(t - t_1)$ $(t > t_1)$.

Within the framework of the general dam-break problem (9.1), the constructed solution of the discontinuity decay problem (9.8) forms a solution consisting of two depression waves (9.11), (9.12) and a discontinuous wave (2.2), (7.7), which are connected by the constant-flow regions (9.7) and (9.10). In Fig. 3b, this solution is shown by solid curve 1, and in Fig. 4, by the curve $h^*G_1G_2F_1F_2x_6$. Since the right boundary F_1 of the depression s-wave (9.12) propagates at the velocity $u_1 + c_1$ higher than the velocity $D = u_1$ of motion of the front F_2x_6 of the discontinuous wave (2.2), this solution exists until the point F_1 (see Fig. 4) "overtakes" the point F_2, i.e., only in the time interval (t_1, t_2), where $t_2 = u_1t_1/c_1$. At $t > t_2$, interaction of the discontinuous wave (2.2) with the depression wave (9.12) begins which is not described by self-similar solutions.

The exact solution of the dam-break problem (9.1), shown by the curve $h^*G_1G_2F_1F_2x_6$ in Fig. 4, depends on two dimensionless parameters: the Froude number θ behind the discontinuous-wave front F_2x_6 and the parameter τ which determines the existence of the depth discontinuity h_1h^*. The results of experimental modeling studies [21, 23] of the dam-break problem (9.1) at initial depths $H_0 = 3$–21 cm, it follows that, at $H_0 = 7$–21 cm, the parameters θ and τ change only slightly and are close to the constant values $\theta = 6.7$ and $\tau = 0.62$. For these values of the parameters θ and τ, the exact solution is in good agreement with the data of the laboratory experiments at $t > kt_1 = k\tau\sqrt{H_0/g}$ $(k = 1.3)$, where the vertical velocities at the dam location decay and the real flow can be considered one-dimensional. Assuming that, in the given problem, the characteristic flow depth H coincides with the initial headwater depth, i.e., $H = H_0$, from formula (7.8), in view of (9.7), we obtain the following value of the dimensionless parameter γ^*:

$$\gamma^* = 4/(9\sqrt[3]{\theta}\,(\theta - 2)) \approx 0.05.$$

From Fig. 3b, it follows that for the time $t = 1.47$ sec $\in (kt_1, t_2)$ $(t_1 \approx 0.77$ sec $\Rightarrow kt_1 \approx 1$ sec; $t_2 \approx 2$ sec), the modified self-similar solution constructed in the present section provides a fairly accurate approximation of the experimental wave profile in the tailwater, which indicates that the assumptions used in its construction are valid. For the earlier time $t = 0.41$ sec $< t_1$ (see Fig. 3a), when the unstable discontinuity $[h_1, h^*]$ has not yet decayed and the real flow is substantially two-dimensional, the calculation results and experimental data are in much worse agreement.

10. Closed System of Equations for Describing Turbulent Bores. To derive the modified total-momentum conservation law (7.2), under which the shallow water equations admit the propagation of discontinuous waves over a dry bed, it is sufficient to specify the dependence of the turbulent viscosity (5.4) ν_* on the vertical velocity component w_* only on the free surface (4.5) of the transition region (4.6.) At the same time, for a more detailed analysis of turbulent flow in this region (turbulent bore), it is necessary to determine dependence (5.4) for all $z^* \in [0, h^*]$ and to specify the explicit form of the free-energy function $\sigma_*(u^*, w_*)$ on the free surface (4.5). This is easy to do by assuming that, as $\delta \to 0$,

$$\nu_* \approx \gamma^* w_* \quad \forall z^* \in [0, h^*], \qquad \sigma_* \approx \vartheta_* w_*^2\Big|_{z^*=h^*} \tag{10.1}$$

($\vartheta_* = H\vartheta/l^2 = \text{const}$). In this case, the dynamic boundary condition (4.19) becomes

$$\Big(\frac{\partial w_*}{\partial x_*} + \frac{\partial w_*}{\partial z^*}\frac{\partial h^*}{\partial x_*} + r_*\frac{\partial u^*}{\partial z^*}\Big)\Big|_{z^*=h^*} = 0, \tag{10.2}$$

where $r_* = \gamma^*/\vartheta_* = \text{const}$. As a result, for the specified dimensionless parameters γ^* and ϑ_*, we obtain the closed system (4.12), (4.18), (4.20) of nonideal vortex shallow water with the following boundary conditions: the nonpenetration condition at the bottom $w_*(x_*, 0, t_*) = 0$, and the kinematic condition (4.16) and dynamic condition (10.2) on the free surface. From the first formula (10.1) it follows that this system ignores the bottom friction effect due to the turbulent viscosity in the near-bottom boundary layer, whose thickness is considered negligible compared to the characteristic flow depth H. This system can be used for numerical modeling of the formation and evolution of turbulent bores.

I thank V. V. Kuznetsov for useful discussions of the work.

This work was supported Program of the President of the Russian Federation on the State Support of Leading Scientific Schools (Grant No. NSh-5873.2006.1), Russian Foundation for Basic Research (Grant No. 07-01-00609) and a project for basic research of the Presidium of the Russian Academy of Sciences (Grant No. 16.2).

REFERENCES

1. J. J. Stoker, *Water Waves Wiley*, New York (1992).
2. L. V. Ovsyannikov, N. I. Makarenko, V. I. Nalimov, et al., *Nonlinear Problems of the Theory of Surface and Internal Waves* [in Russian], Nauka, Novosibirsk (1985).
3. V. Yu. Liapidevskii and V. M. Teshukov, *Mathematical Models for Propagation of Long Waves in an Inhomogeneous Fluid* [in Russian], Izd. Sib. Otd. Ross. Akad. Nauk, Novosibirsk (2000).
4. A. G. Kulikovskii, N. V. Pogorelov, and A. Yu. Semenov, *Mathematical Questions of Numerical Solution of Hyperbolic Systems of Equations* [in Russian], Fizmatlit, Moscow (2001).
5. V. V. Ostapenko, *Hyperbolic Systems of Conservation Laws and Their Applications to Shallow Water Theory* [in Russian], Izd. Novosibirsk Gos. Univ., Novosibirsk (2004).
6. O. F. Vasil'ev and M. T. Gladyshev, "Calculation of discontinuous waves in open channels," *Izv. Akad. Nauk SSSR, Mekh. Zhidk. Gaza*, No. 6, pp. 120–123 (1966).
7. V. V. Ostapenko, "Through calculation of discontinuous waves," *Zh. Vychisl. Mat. Mat. Fiz.*, **33**, No. 5, 743–752 (1993).
8. A. F. Voevodin and V. V. Ostapenko, "Calculation of discontinuous waves in open channels," *Sib. Zh. Vychisl. Mat.*, **3**, No. 4, 305–321 (2000).
9. A. Delis and C. P. Skeels, "TVD schemes for open channel flow," *Int. J. Numer. Methods Fluids*, **26**, 791–809 (1998).
10. J. Wang, H. Ni, and Y. Ni, "Finite-difference TVD schemes for computation of dam-break problems," *J. Hydraul. Eng. ASCE*, **126**, 253–262 (2000).
11. G. Gottardi and M. Venutelli, "Central schemes for open channel flow," *Int. J. Numer. Methods Fluids*, **41**, 841–861 (2003).
12. Yu. I. Shokin, L. B. Chubarov, A. G. Marchuk, and K. V. Simonov, *Computational Experiment in the Tsunami Problem* [in Russian], Nauka, Novosibirsk (1989).
13. A. Ritter, "Die fortpflanzung der wasserwellen," *Z. Vereins Ing.*, **36**, 947–954 (1892).
14. R. F. Dressler, "Hydraulic resistance effect upon the dam-break functions," *J. Res. Nat. Bureau Standards*, **49**, No. 3, 217–225 (1952).
15. G. B. Whitham, "The effects of hydraulic resistance in the dambreak problem," *Proc. Roy. Soc. London, Ser. A*, **227**, No. 1170, 399–407 (1955).
16. V. G. Sudobicher and S. M. Shugrin, "Motion of a water flow over a dry bed," *Izv. Akad. Nauk SSSR, Ser. Tekh. Nauk*, **13**, No. 3, 116–122 (1968).

17. N. M. Borisova and V. V. Ostapenko, “Numerical modeling of discontinuous-wave propagation over a dry bed,” *Zh. Vychisl. Mat. Mat. Fiz.*, **46**, No. 7, 1322–1344 (2006).
18. J. C. Martin and W. J. Moyce, “An experimental study of the collapse of liquid columns on a rigid horizontal plane,” *Philos. Trans. Roy. Soc. London, Ser. A*, **244**, 312–324 (1952).
19. R. F. Dressler, “Comparison of theories and experiments for the hydraulic dam-break wave,” *Int. Assoc. Sci. Hydrology*, **3**, No. 38, 319–328 (1954).
20. P. K. Stansby, A. Chegini, and T. C. Barnes, “The initial stages of dam-break flow,” *J. Fluid Mech.*, **374**, 407–424 (1998).
21. V. I. Bukreev, A. V. Gusev, A. A. Malysheva, and I. A. Malysheva, “Experimental verification of the gas-hydraulic analogy by the example of the dam-break problem,” *Izv. Ross. Akad. Nauk, Mekh. Zhidk. Gaza.*, **5**, 143–152 (2004).
22. V. I. Bukreev and A. V. Gusev, “Initial stage of generation of dam-break waves,” *Dokl. Ross. Akad. Nauk*, **401**, No. 5, 1–4 (2005).
23. N. M. Borisova, A. V. Gusev, and V. V. Ostapenko, “Propagation of discontinuous waves over a dry bed,” *Izv. Ross. Akad. Nauk, Mekh. Zhidk. Gaza.*, **4**, 135–148 (2006).
24. K. O. Friedrichs and P. D. Lax, “Systems of conservation equation with convex extension,” *Proc. Nat. Acad. Sci. USA*, **68**, No. 8, 1686–1688 (1971).
25. P. D. Lax, *Hyperbolic Systems of Conservation Laws and the Mathematical Theory of Shock Waves*, Soc. Industr. and Appl. Math., Philadelphia (1972).
26. K. O. Friedrichs, “On the derivation of shallow water theory,” *Comm. Pure Appl. Math.*, **1**, 109–134 (1948).
27. A. A. Atavin and S. M. Shugrin, “Differential equations of shallow water theory,” in: *Dynamics of Continuous Media* (collected scientific papers) [in Russian], No. 70, Inst. of Hydrodynamics, Sib. Div., Acad. of Sci. of the USSR, Novosibirsk (1985), pp. 25–53.
28. V. V. Pukhnachev, *Motion of a Viscous Fluid with Free Boundaries* [in Russian], Izd. Novosibirsk Gos. Univ., Novosibirsk (1989).
29. P. A. Madsen and I. A. Svedsen, “Turbulent bores and hydraulic jumps,” *J. Fluid Mech.*, **129**, 1–25 (1983).
30. I. A. Svedsen and P. A. Madsen, “Turbulent bore on a beach,” *J. Fluid Mech.*, **148**, 73–96 (1984).
31. J. W. Hoyt and R. H. Sellin, “Hydraulic jumps as ‘mixing layer’,” *J. Hydraul. Eng.*, **115**, No. 12, 1607–1614 (1989).
32. M. Gunal and R. Narayanan, “Hydraulic jump in sloping beds,” *J. Hydraul. Eng.*, **122**, No. 8, 436–442 (1996).
33. N. C. Freeman, “Simple waves on shear flow: similarity solutions,” *J. Fluid Mech.*, **56**, 257–263 (1972).
34. D. J. Benney, “Some properties of long nonlinear waves,” *Stud. Appl. Math.*, **52**, 45–50 (1973).
35. V. E. Zakharov, “Benney equations and quasi-classical approximation in the method of inverse problem,” *Funct. Anal. Appl.*, **14**, 15–24 (1980).
36. P. L. Sachdev and Ph. Varugheze, “Invariance group properties and exact solutions of equations describing time-dependent free surface flow under gravity,” *Quart. Appl. Math.*, **43**, 465–482 (1986).
37. V. Teshukov, G. Russo, and A. Chesnokov, “Analytical and numerical solutions of the shallow water equations for 2D rotational flows,” *Math. Models Methods Appl. Sci.*, **14**, No. 10, 1451–1479 (2004).